

Hydrogen-Bond-Mediated Photoinduced Electron-Transfer: Novel Dimethylaniline–Anthracene Ensembles Formed via Watson–Crick Base-Pairing

Jonathan L. Sessler,^{*,†} Muhunthan Sathiosatham,[†] Christopher T. Brown,[†] Timothy A. Rhodes,[‡] and Gary Wiederrecht^{*,§}

Contribution from the Department of Chemistry and Biochemistry, University of Texas at Austin, Austin, Texas 78712, Center for Photoinduced Electron-Transfer, University of Rochester, Rochester, New York 14618, and Chemistry Division, Argonne National Laboratory, Chicago, Illinois 60439

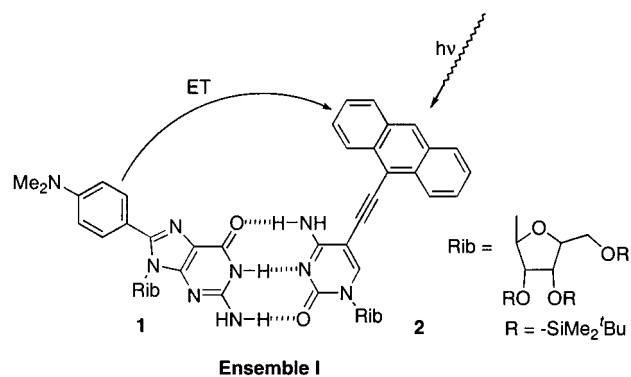
Received August 24, 2000. Revised Manuscript Received February 15, 2001

Abstract: The synthesis of a new, noncovalent anthracene–dimethylaniline dyad (ensemble **I**) held together via guanosine–cytidine Watson–Crick base-pairing interactions is reported. Upon excitation at 420 nm, photoinduced electron-transfer from the dimethylaniline donor to the singlet excited state of the anthracene acceptor occurs, as inferred from a combination of time-resolved fluorescence quenching and transient absorption measurements. In toluene at room temperature, the rate constants for photoinduced intraensemble electron-transfer and subsequent back-electron-transfer (charge recombination) are $k_{CS} = (3.5 \pm 0.03) \times 10^{10} \text{ s}^{-1}$ and $k_{CR} = (1.42 \pm 0.03) \times 10^9 \text{ s}^{-1}$, respectively.

Introduction

Noncovalent interactions play a critical role in mediating a range of biological electron-transfer (ET) processes both thermal and photoinduced.¹ While subject to considerable theoretical² and experimental³ scrutiny, the fundamental principles of how such interactions might serve to mediate ET reactions remain recondite. For this reason we,⁴ and others,⁵ have been keen to develop simple model systems that would allow the underlying chemical and photochemical events to be probed with greater precision. In this context, particular attention has been focused on self-assembled ensembles formed via H-bonds.^{4,5} Our approach to this problem has involved the use of Watson–Crick base pairing as a mean of (1) establishing the critical donor–

Chart 1



acceptor interactions (i.e., ensemble formation) and (2) providing pathways for possible intraensemble electron- or energy-transfer (i.e., putting in place a critical matrix coupling element).⁴ While a number of such systems have been introduced, in no case was direct evidence for charge separation obtained under conditions of simple solution-phase photoexcitation.⁶ Here, we report the synthesis and photophysical characterization of a dimethylaniline–anthracene ET model system (ensemble **I**) in which both photoinduced charge separation and subsequent thermal charge recombination were directly observed via transient absorption spectroscopy.

Results and Discussion

Synthesis. Scheme 1 illustrates the synthesis of donor **1** and acceptor **2**. Briefly, the protected donor **5** was synthesized from known compounds **3**⁷ and **4**⁸ in 85% yield via Stille cross-

[†] University of Texas at Austin.

[‡] University of Rochester.

[§] Argonne National Laboratory.

(1) Sessler, J. L.; Wang, B.; Springs, S. L.; Brown, C. T. In *Comprehensive Supramolecular Chemistry*; Murakami, Y., Ed.; Pergamon: New York, 1996; Vol. 4, pp 311–336 and references therein.

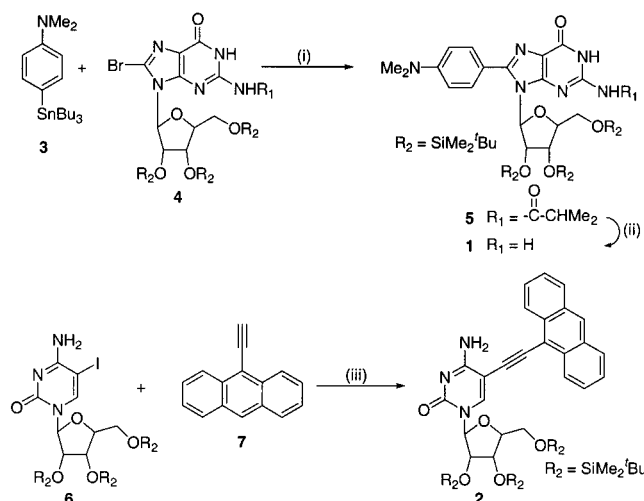
(2) (a) Marcus R. A. *J. Phys. Chem. B* **1998**, *102*, 10071–10077 and references therein. (b) Marcus, R. A.; Sutin N. *Biochim. Biophys. Acta* **1985**, *811*, 265–322.

(3) (a) Babini, E.; Bertini, I.; Borsari, M.; Capozzi, F.; Luchinat, C.; Zhang, X.; Moura, G. L. C.; Kurnikov, I. V.; Beratan, D. N.; Adrian, P.; Di Bilio, A. J.; Winkler, J. R.; Gray, H. B. *J. Am. Chem. Soc.* **2000**, *122*, 4532–4533. (b) Nocek, J. M.; Zhou, J. S.; Forest, S. D.; Priyadarshy, S.; Beratan, D. N.; Onuchic, J. N.; Hoffman, B. M. *Chem. Rev.* **1996**, *96*, 2459–2489 and references therein.

(4) (a) Berg, A.; Shuali, Z.; Asano-Someda, M.; Levanon, H.; Mobius, K.; Fuhs, M.; Wang, R.; Brown, C. T.; Sessler, J. L. *J. Am. Chem. Soc.* **1999**, *121*, 7433–7434. (b) Sessler, J. L.; Brown, C. T.; O'Connor, D.; Springs, S. L.; Wang, R.; Sathiosatham, M.; Hirose, T. *J. Org. Chem.* **1998**, *63*, 7370–7374. (c) Sessler, J. L.; Wang, B.; Harriman, A. *J. Am. Chem. Soc.* **1993**, *115*, 10418–10419.

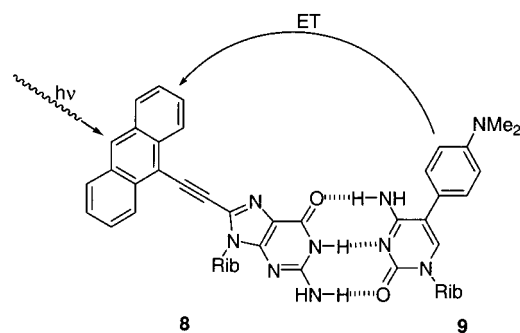
(5) (a) Ghaddar, T. H.; Castner, E. W.; Isied, S. S. *J. Am. Chem. Soc.* **2000**, *122*, 1233–1234. (b) Williamson, D. A.; Bowler, B. E. *J. Am. Chem. Soc.* **1998**, *120*, 10902–10911. (c) Osuka, A.; Yoneshima, R.; Shiratori, H.; Okada, T.; Taniguchi, S.; Mataga, N. *Chem. Commun.* **1998**, 1567–1568. (d) Deng, Y.; Roberts, J. A.; Peng, S.-M.; Chang, C. K.; Nocera, D. G. *Angew. Chem., Int. Ed. Engl.* **1997**, *36*, 2124–2127. (e) Kirby, J. P.; Roberts, J. A.; Nocera, D. G. *J. Am. Chem. Soc.* **1997**, *119*, 9230–9236.

(6) Evidence for ET was, however, obtained by EPR measurements carried out in liquid crystalline media, see: Berman, A.; Izraeli, E. S.; Levanon, H.; Wang, B.; Sessler, J. L. *J. Am. Chem. Soc.* **1995**, *117*, 8252–8257.

Scheme 1^a

^a Reagents: (i) Pd(PPh₃)₄, toluene, reflux, 12 h, 85%; (ii) NH₃, MeOH, DCM, room temperature, 48 h, 70%; (iii) Pd(PPh₃)₂Cl₂, CuI, ^tPr₂NH, room temperature, 6 h, 80%.

Chart 2



Ensemble II

coupling. The desired donor **1** was obtained in 70% yield by treating **5** with ammonia-saturated MeOH/CH₂Cl₂ at room temperature. The synthesis of acceptor **2** was accomplished in 80% yield by carrying out a Sonagashira cross-coupling between the known compounds **6**⁹ and **7**.¹⁰ Scheme 2 summarizes the chemistry used to prepare **8** and **9**, the key components needed to generate ensemble II (Chart 2). Briefly, the *N*-protected acceptor **10** was synthesized in 87% yield from **4**⁸ and **7**¹⁰ by using Sonagashira cross-coupling. As above, the desired acceptor, **8** in this instance, was then obtained by treating **10** with ammonia-saturated MeOH/CH₂Cl₂ at room temperature (yield 60%). The donor **9** was synthesized in 50% yield by carrying out a Negishi cross-coupling between the organozinc intermediate **12** and known precursor **6**.⁹

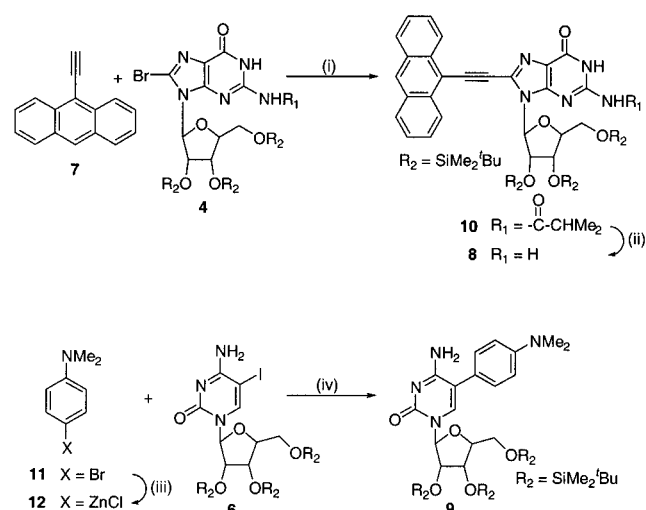
Molecular Recognition. Proton NMR spectroscopic analyses of ensemble I were carried out under conditions analogous to those used for subsequent photophysical analysis, and were used to confirm the presence of Watson–Crick type molecular recognition. Here, rather than carrying out standard ¹H NMR titrations, we used the dilution method developed by Creswell and Allred,¹¹ from which estimates of the association constant (*K*_a) corresponding to the formation of ensemble I could be

(7) Farina, V.; Krishnan, B.; Marshall, D. R.; Roth, G. P. *J. Org. Chem.* **1993**, *58*, 5434–5444.

(8) Nagatsugi, F.; Uemura, K.; Nakashima, S.; Maeda, M.; Sasaki, S. *Tetrahedron* **1997**, *53*, 3035–3044.

(9) Nguyen, P.; Todd, S.; Van den Biggelaar, D.; Taylor, N. J.; Marder, T. B.; Wittmann, F.; Friend, R. H. *Synlett* **1994**, 299–301.

(10) Sessler, J. L.; Wang, R. *J. Org. Chem.* **1998**, *63*, 4079–4091.

Scheme 2^a

^a Reagents: (i) Pd(PPh₃)₂Cl₂, CuI, ^tPr₂NH, room temperature, 6 h, 87%; (ii) NH₃, MeOH, DCM, room temperature, 48 h, 60%; (iii) (a) BuLi, THF, −78 °C, 0.5 h; (b) ZnCl₂, THF, −78 °C → room temperature; (iv) Pd(PPh₃)₄, toluene, reflux, 12 h, 50%

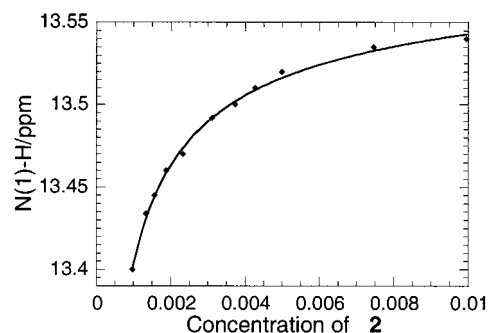


Figure 1. ¹H NMR binding profiles corresponding to the formation of ensemble I from **1** and **2**. Analysis (see text) confirms the expected 1:1 binding stoichiometry and gives a dissociation constant, *K*_d, of $(2.6 \pm 0.09) \times 10^{-5}$ M, corresponding to an association constant, *K*_a, of 38500 ± 1300 M^{−1}.

derived. These experiments, carried out in CD₂Cl₂ solution, confirmed the expected 1:1 stoichiometry. Nonlinear regression analyses of the data also yielded a *K*_a of 38000 ± 1300 M^{−1}. Such a *K*_a value is higher than those seen for previous Watson–Crick ensembles,^{4c} a difference we ascribe to the increased rigidity of the individual components present in ensemble I as compared to those present in earlier systems.

Energetics of the PET. Once evidence for ensemble formation was obtained, the energetics of dyad I, containing donor **1** and acceptor **2**, were determined from a combination of ground-state absorbance, steady-state emission, and square-wave voltammetric analyses. From these measurements, carried out in accord with standard literature procedures,¹² the driving force for the putative intraensemble dimethylaniline-to-photoexcited anthracene photoinduced electron-transfer (PET) charge separation ($\Delta G_{CS}^0 = -0.41$ eV) and follow-up charge recombination ($\Delta G_{CR}^0 = -2.5$ eV) processes were estimated.

Fluorescence Quenching. Initial experimental support for the proposed intraensemble PET process came from steady-

(11) (a) Creswell, C. J.; Allred, A. L. *J. Phys. Chem.* **1962**, *66*, 1469–1472. (b) Wilcox, C. W. In *Frontiers in Supramolecular Organic Chemistry and Photochemistry*; Schneider, H.-J., Durr, H., Eds.; VCH: Weinheim, 1991; pp 123–143.

(12) (a) Kavarnos, G. J.; Turro, N. J. *Chem. Rev.* **1986**, *86*, 401–449. (b) Rehm, D.; Weller, A. *Isr. J. Chem.* **1970**, *8*, 259–271.

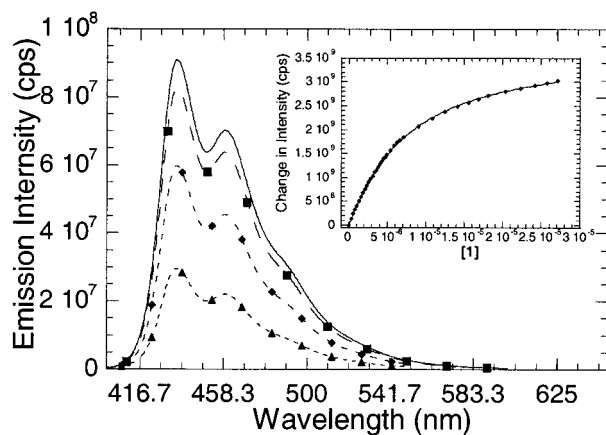


Figure 2. Steady-state fluorescence changes accompanying the titration of acceptor **2** (5.2×10^{-6} M) with donor **1**. The donor **1** concentrations are the following: (—) 0.0 M, (■) 1.0 μ M, (◆) 5.0 μ M, and (▲) 30 μ M. Inset: Plot of change in integrated fluorescence intensity (◆) of acceptor **2** as a function of donor concentration. The solid line represents the estimated curve obtained by nonlinear least-squares analysis using the algorithms developed elsewhere.¹⁴ This titration was carried out in CH_2Cl_2 and excitation was effected at 408 nm.

state fluorescence quenching measurements. Here, the steady-state fluorescence properties of **2** (5.0×10^{-6} M) were monitored as a function of [1] in toluene and CH_2Cl_2 . The fluorescence intensity of acceptor **2**, ascribed to singlet state emission from the photoexcited anthracene chromophore, was quenched significantly upon increasing concentration of acceptor **1** (cf., Figure 2). The extent of such quenching began to level off after the addition of approximately 1 molar equiv of **1** (cf., Figure 2, Inset). This observation contrasts greatly with what is seen in the case of simple anthracene and dimethylaniline. In this latter instance, only 2% of the anthracene-based fluorescence intensity is quenched at similar absolute and relative concentrations of dimethylaniline.¹³ The same lack of substantial quenching was also observed when acceptor **2** was mixed with the “masked donor” **5**, wherein the hydrogen bond donor NH_2 group is blocked.¹³ On this basis, we therefore conclude that diffusion-controlled (Stern–Volmer type) collisions cannot account for the large degree of quenching observed when **2** is exposed to small amounts of **1**. Rather we propose that hydrogen-bond-mediated electron-transfer within ensemble **I** is responsible.

Time-Resolved Fluorescence Measurements. Time-resolved fluorescence lifetime measurements were used to estimate the rate of ET from the donor **1** to excited acceptor **2** in CH_2Cl_2 . Specifically, after photoexcitation at 420 nm, the emission of **2**, monitored at 440 nm as a function of time in the presence of **1**, displayed a fast rise, ascribed to the formation of the singlet excited state of the anthracene chromophore, followed by a biexponential decay (cf., Figure 3). Such a decay profile, observed for analogous ET ensembles,^{4c,5a} is interpreted in terms of a linear combination of two fluorescing species, namely the excited singlet state of the uncomplexed acceptor **2** (longer lifetime; τ_0) and photoexcited acceptor **2** held within ensemble **I** (shorter lifetime; τ_1). Assuming the shorter lifetime process reflects efficient quenching as the result of fast intraensemble ET from donor **1** to photoexcited **2**, a rate constant for ET of $k_{\text{CS}} = (1.3 \pm 0.1) \times 10^{10} \text{ s}^{-1}$ could be estimated according to $k_{\text{CS}} = [(1/\tau_0) - (1/\tau_1)]$. Further, from standard Marcus-type analyses of forward electron-transfer rates (k_{CS}) measured at

(13) See Supporting Information for details.

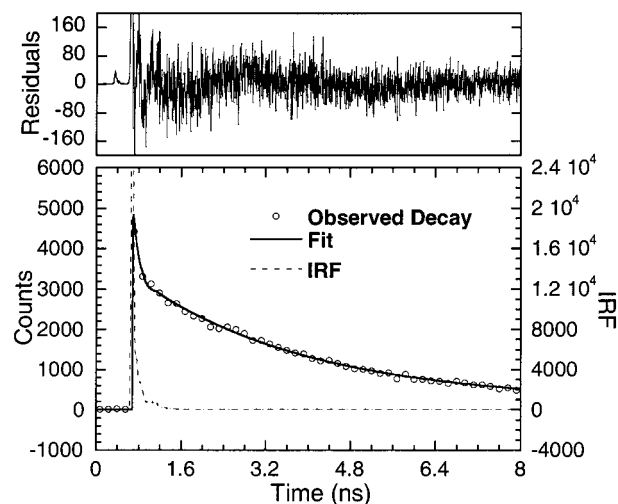


Figure 3. Decay profile and residual curve fitting for the time-resolved fluorescence of acceptor **2** (4.1×10^{-6} M in CH_2Cl_2) observed in the presence of donor **1** (5.24×10^{-6} M). Apart from an instrument limited photoexcitation process, curve fitting revealed a biexponential decay with $\tau_0 = 3.23 \pm 0.017$ ns and $\tau_1 = 77.5 \pm 8.6$ ps. Excitation was effected with 70 ps 420 nm laser pulses, with emission being monitored at 440 nm. Data were collected over 10 ns with a time calibration of 0.004 ns/channel.

different temperatures,¹⁵ a reorganization energy, λ_{el} , of ca. 1.0 eV and an electronic matrix coupling energy, H_{DA} , of ca. 130 cm^{-1} could be derived. While this value is high compared to our previous Watson–Crick systems,^{4c} for which an H_{DA} value of 33 cm^{-1} was observed, it is consistent with the basic premise of this work, namely that, within the context of ensemble **I**, donor **1** should be very effective at quenching the excited state of acceptor **2** via direct electron-transfer.¹⁶

Femtosecond Transient Absorption Spectroscopic Measurement. Additional support for the contention that the excited anthracene moiety of acceptor **2** was quenched due to intraensemble ET from donor **1** came from transient absorption spectroscopic analyses carried out in toluene. Here, a solution of acceptor **2** and donor **1** at room temperature was excited with 150 fs 417 nm laser pulses with the resulting changes in the absorption profile between 450 and 750 nm being monitored as a function of time (cf., Figure 4). A strong absorption at 590 nm, ascribed to the $S_n \leftarrow S_1$ transition of the anthracene moiety in acceptor **2**, was observed 15 ps after photoexcitation. This band then decayed over the course of roughly 150 ps while concurrently a new absorption band was seen to grow in at 480 nm. This latter band was assigned, on the basis of literature precedent,¹⁷ to the radical cation of dimethylaniline, produced as the result of ET to photoexcited acceptor **2**. Following the time course of the absorption band at 590 nm revealed, in analogy to what was seen in the time-resolved fluorescence studies, a fast rise process followed by a biexponential decay. The faster of these decays was again considered to reflect

(14) (a) Popieniek, P. H.; Pratt, R. F. *Anal. Biochem.* **1987**, *165*, 108–113. (b) Lacourciere, K. A.; Stivers, J. T.; Marino, J. P. *Biochemistry* **2000**, *39*, 5630–5641.

(15) Fluorescence lifetimes measured at different temperatures were used to estimate the PET rate constant. See Supporting Information for plot of $k_{\text{ET}}\sqrt{T}$ vs $1/T$. For the specific form of the Marcus equation employed see eq 18a in: Bolton, J. R.; Archer, M. D. *Adv. Chem. Ser.* **1991**, *228*, 7–23.

(16) Consistent with this thinking is the finding that the rate of electron-transfer, k_{CS} , observed in ensemble **I** is ca. an order of magnitude greater than that in our previous Watson–Crick model systems.^{4c}

(17) (a) Mataga, N.; Nishikawa, S.; Asahi, T.; Okada, T. *J. Phys. Chem.* **1990**, *94*, 1443–1447. (b) Mataga, N. *Adv. Chem. Ser.* **1991**, *228*, 91–115.

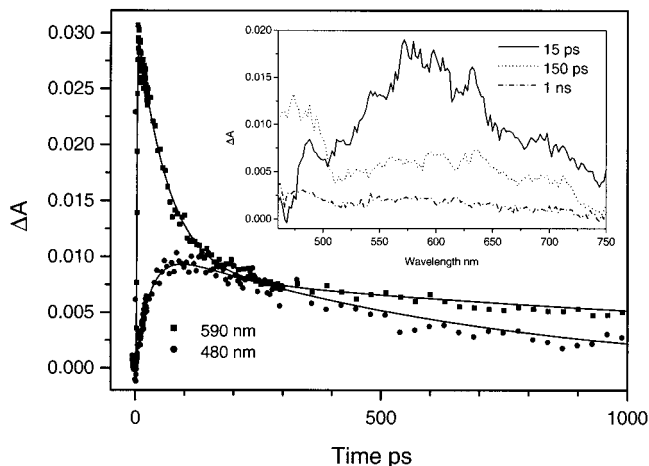


Figure 4. Transient absorption kinetics monitored at 590 (■) and 480 nm (●) for a solution of acceptor **2** (2.3×10^{-5} M) and donor **1** (6.8×10^{-4} M) in toluene at room temperature. Excitation was effected with $0.05 \mu\text{J}$, 150 fs, 417 nm laser pulses. Inset: Spectra were recorded after probe delays of 15, 150, and 500 ps. The solution was degassed by subjecting it to a freeze–pump–thaw cycle.

intraensemble ET. Kinetic analyses of the 590 nm band gave an approximate rate constant for charge separation, k_{CS} , of $(2 \pm 0.5) \times 10^{10} \text{ s}^{-1}$, a value that compares favorably with that obtained from time-resolved fluorescence studies. On the other hand, monitoring the absorption band at 480 nm revealed a rise ($\tau_{\text{R}} = 29.0 \pm 1.0$ ps) followed by a monoexponential decay ($\tau_{\text{D}} = 705.0 \pm 20.0$ ps). From these, the rate constant for forward ET [$k_{\text{CS}} = (3.5 \pm 0.03) \times 10^{10} \text{ s}^{-1}$] and the back ET [$k_{\text{CR}} = (1.42 \pm 0.03) \times 10^9 \text{ s}^{-1}$], representing the formation (rise) and disappearance (decay) of the dimethylaniline cation radical of donor **1**, were calculated. These compare favorably with but are slightly slower than those seen in various covalently linked dimethylaniline–anthracene ET model systems.^{17,18} This leads to the suggestion that the hydrogen-bonded bridges present in **I** are playing a critical role in mediating the ET process, either as the result of establishing a supramolecular ensemble with favorable donor–acceptor distance and orientations or as a result of providing a direct, favorable through H-bond pathway for ET, or both.¹⁹

Reversed Ensemble. To obtain further insights into the role the hydrogen-bonding linker elements play in mediating the behavior of ensemble **I**, the “reversed” electron-transfer ensemble **II** ($\Delta G^\circ = -0.33$ eV) was constructed (see Chart 2). The synthesis of the key components of this ensemble, namely acceptor **8** and donor **9**, is summarized in Scheme 2, with full details being provided in the Experimental Section.

In the case of ensemble **II**, steady-state fluorescence analyses of the acceptor (**8**; 1.3×10^{-6} M in CH_2Cl_2) carried out in the presence of the donor (**9**) revealed not only significant quenching (as seen with ensemble **I**) but also the production of exciplex-type spectral features (cf., Figure 5). This behavior, fully manifest at a donor/acceptor ratio of 1:1, contrasts greatly with

(18) Although comparisons of this type are necessarily far from ideal, they have been used frequently to obtain insights into the nature and properties of noncovalent ET model systems. For example, see refs 5a, 5c, and de Rege et al.: de Rege, P. J. F.; Williams, S. A.; Therien, M. J. *Science* **1995**, 269, 1409–1413.

(19) Transient absorption spectrum recorded after the addition of 5% methanol to the same solution displayed a monoexponential decay at 590 nm and failed to show any absorption at 480 nm. Methanol is known to compete for the hydrogen-bonding sites and disrupt association. The results of this control experiment further underscore the importance of hydrogen bonding in establishing directly or indirectly the ET dynamics of ensemble **I**.

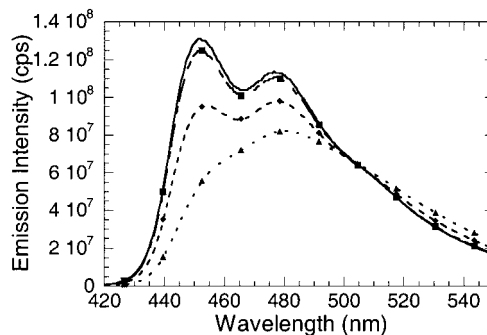


Figure 5. Steady-state fluorescence changes accompanying the titration of acceptor **8** (1.3×10^{-5} M) with donor **9**. The donor **9** concentrations are the following: (—) 0.0 M, (■) 1.0 μM , (●) 5.0 μM , and (▲) 13 μM . This titration was carried out in CH_2Cl_2 and excitation was effected at 388 nm.

that seen in the case of ensemble **I**. Such behavior, based on available literature precedence,²⁰ was initially thought to reflect π -stacking interactions involving the anthracene acceptor **8** and the dimethylaniline donor **9**. On the other hand, simple control experiments that involved carrying out a fluorescence titration of acceptor **8** with donor **9** at an order of magnitude lower initial concentration (of **8**) revealed similar exciplex-type emission. Further, fluorescence quenching experiments conducted using the “masked acceptor” **10** in lieu of **8** (as well as, of course, **9**) did not yield any evidence for the formation of an exciplex type emission. Taken together, these observations lead us to rule out π -stacking and other forms of intermolecular aggregation as reasonable explanations for the exciplex-type emission observed in the case of ensemble **II**. On the other hand, the addition of methanol, a solvent known to disrupt hydrogen-bonding, to solutions of **8** and **9** was found to restore, at least in large measure, the classic anthracene-type emission seen for pure solutions of **8**. These findings are consistent with the observed exciplex-type emission being an intrinsic feature of the hydrogen-bonded ensemble **II**. On the other hand, they do not serve to explain why ensemble **II** differs so greatly in its photophysical properties from ensemble **I**. In an effort to probe this issue further, CW emission and transient absorption studies of ensemble **II** were carried out in toluene. Here, in contrast to what was seen in the case of ensemble **I**, no evidence of photoinduced charge separation was obtained. In other words, under these conditions, **9** was not seen to quench the normal anthracene emission of **8**.

Conclusions

At present, the reasons for the difference between ensembles **I** and **II** are not fully understood. Our current hypothesis, fully consistent with related proposals in the literature,^{5c,21} is that not only is the choice of a given type of donor–acceptor linking element important in terms of mediating long-range ET events but also more subtle issues, such as linker orientation, configuration, and (as in the case of ensembles **I** and **II**) directionality play a critical key role in influencing donor–acceptor interactions. Driving force differences could also be important, with that of ensemble **II** being estimated at ca. 0.08 eV less than that of ensemble **I**.

In a more general sense, the present studies serve to underscore that in the specific case of Watson–Crick-type

(20) Turro, N. J. *Modern Molecular Photochemistry*; University Science Books: Sausalito, 1991; pp 136–145.

(21) Kuciaukas, D.; Liddell, P. A.; Hung, S.-C.; Lin, S.; Stone, S.; Seely, G. R.; Moore, A. L.; Moore, T. A.; Gust, D. J. *Phys. Chem. B* **1997**, 101, 429–440.

noncovalent electron-transfer model systems, intraensemble electron-transfer processes can be fast and facile and readily observable by transient absorbance methods (cf., ensemble **I**). However, as evidenced by ensemble **II**, this need not always be the case. This disparity illustrates in cogent fashion the importance of careful design when seeking to generate new noncovalent ET model systems.

Experimental Section

General Information. ^1H and ^{13}C NMR spectra were recorded on General Electric QE-300 MHz, Varian Gemini 300 or 500 MHz, or Bruker 500 MHz NMR spectrometers using the residual peaks of deuterated solvents as internal standards. UV/visible spectra were obtained using a Beckman DU 540 spectrophotometer. Fluorescence spectral measurements were carried out on a SPEX-332 spectrofluorimeter. Cyclic voltammetric measurements were made on a BAS MF 9093 CV ~ 50 W Version 2 instrument. The working electrode was a Pt disk with a Pt wire as the counter electrode, and the reference electrode was Ag/AgCl. All measurements were carried out with 0.15 M tetrabutylammonium hexafluorophosphate as the supporting electrolyte. Low-resolution (LR) chemical ionization (CI) mass spectra (MS) were measured using either a Finnigan-MAT 4023 or a Howell 21-491 spectrometer. High-resolution mass spectra (HRMS) were recorded on a Bell and Howell 21-110B mass spectrometer.

The time-resolved picosecond fluorescence lifetime measurements were carried out at The Center for Photoinduced Electron-Transfer Facility at The University of Rochester. The equipment description of the system has been reported previously.¹ The excitation was effected with 70 ps 420 nm pulses and the emission was monitored at 440 nm.

The femtosecond transient absorption measurements were carried out at the Argonne National Laboratory on a system that has been previously described.² Briefly, the amplified output of a Ti:sapphire laser (300 μJ , 835 nm) was split and 95% was frequency doubled to serve as the pump (excitation) beam. Samples were typically excited with 0.05–1.0 μJ , 150 fs, 417 nm pulses. The remaining 5% of the amplified 835 nm light was used to generate a white light continuum probe by focusing into a piece of sapphire. The probe beam was polarized at the magic angle (54.7°) with respect to the pump beam. Amplified photodiodes were used to detect single wavelengths of the probe light after it passed through a monochromator (SPEX model 270M). The photodiode outputs were digitized and recorded using a PC. Multiexponential rise and decay profiles associated with the raw experimental data were fit using the Levenberg–Marquardt algorithm.^{2a}

Materials. Tetrahydrofuran and toluene were distilled over sodium–potassium amalgam. Acetonitrile, dichloromethane, methanol, and diisopropylamine were distilled over calcium hydride. Pyridine was distilled over barium oxide and calcium hydride. Anhydrous *N,N*-dimethylformamide was purchased from Aldrich Chemical Co. and used as received. B & J electro analytical grade acetonitrile and spectroscopic grade dichloromethane were used for electrochemical and photochemical studies, respectively. HPLC grade dichloroethane was used in VPO measurements. All other solvents were reagent grade and used as received. All the starting materials and reagents were purchased from Aldrich, Sigma, and Farchen chemical companies and used as received. TLC analyses were performed on precoated silica gel plates purchased from Whatman International, Inc. Flash chromatography was performed using Merck silica gel 60 as the solid support.

8-(4'-*N,N*-Dimethylaniliny)-9-[2',3',5'-tri-*O*-(*tert*-butyldimethylsilyl)ribofuranosidyl]-2-isobutyrylamidopurin-6-one (5**).** A solution of **3**³ (0.90 g, 2.1 mmol) and **4**⁴ (0.55 g, 0.71 mmol) in dry toluene (50 mL) was purged with argon for 20 min. To this solution was added Pd(PPh₃)₄ (0.1 g, 0.08 mmol) all at once and the resulting solution was heated at reflux under argon for 12 h. After this time, TLC analysis (1:1 ethyl acetate/hexanes) indicated the complete consumption of **5**. The solvent and other volatiles were evaporated off in vacuo. The crude product obtained this way was then purified by flash column chromatography (silica gel, gradient eluent 1:2–2:1 ethyl acetate/hexanes) to afford **5** (0.5 g, 87%). ^1H NMR (300 MHz; CDCl₃): δ -0.27 (s, 3 H), -0.06 (s, 3 H), -0.01 (s, 3 H), 0.04 (s, 3 H), 0.16 (s, 3 H), 0.17 (s, 3 H), 0.8 (s, 9 H), 0.85 (s, 9 H), 0.96 (s, 9 H), 1.26 (d, J = 3.4 Hz, 3 H),

1.28 (d, J = 3.5 Hz, 3 H), 2.64 (m, 1 H), 3.02 (s, 6 H), 3.82 (m, 1 H), 3.95 (m, 2 H), 4.47 (dd, J = 2.2, 4.3 Hz, 1 H), 5.17 (t, J = 5.0 Hz, 1 H), 6.02 (d, J = 6.2 Hz, 1 H), 6.72 (d, J = 8.8 Hz, 2 H), 7.69 (d, J = 8.8 Hz, 2 H), 8.05 (bs, 1 H), 12.00 (bs, 1 H); ^{13}C NMR (125.5 MHz, CDCl₃): δ -5.31, -5.04, -4.62, -4.45, -4.32, 17.90, 18.03, 18.86, 19.06, 25.67, 25.86, 36.67, 40.18, 62.57, 72.00, 72.20, 84.62, 88.73, 111.63, 130.90, 145.70, 151.36, 152.31, 155.20, 177.41. HRMS-CI m/z ($M + 1$) calcd 815.4743, found 815.4732.

8-(4'-*N,N*-Dimethylaniliny)-9-[2',3',5'-tri-*O*-(*tert*-butyldimethylsilyl)ribofuranosidyl]-2-aminopurin-6-one (1**).** An ice-cold mixture of MeOH/CH₂Cl₂ (3:1; 300 mL) was saturated with ammonia gas. This saturation procedure, including careful bubbling, was repeated twice. To the resulting solution was added **5** (0.55 g, 0.67 mmol) with the clear solution that ensued then being stirred at room temperature for 36 h in a sealed flask. The solvents were evaporated off in vacuo. The resulting residue was then purified by flash chromatography (silica gel, eluent 3% MeOH in dichloromethane) to afford **1** (3 g, 50%). ^1H NMR (500 MHz, CDCl₃): δ -0.29 (s, 3 H), -0.09 (s, 3 H), -0.01 (s, 3 H), 0.004 (s, 3 H), 0.07 (s, 3 H), 0.09 (s, 3 H), 0.74 (s, 9 H), 0.85 (s, 9 H), 0.88 (s, 9 H), 2.65 (bs, 1 H), 3.00 (s, 3 H), 3.72 (dd, J = 3.1, 8.9 Hz), 3.90–3.96 (m, 2 H), 4.42 (d, J = 2.2 Hz, 1 H), 5.40 (dd, J = 4.6, 6.0 Hz, 1 H), 5.86 (d, J = 6.3 Hz, 1 H), 6.55 (bs, 1 H), 6.71 (d, J = 8.9 Hz, 2 H), 7.57 (d, J = 8.9 Hz, 2 H), 12.31 (bs, 1 H); ^{13}C NMR (125 MHz, CDCl₃): δ -5.38, -5.34, -5.00, -4.66, -4.55, -4.40, 17.93, 18.01, 18.72, 25.77, 25.84, 25.88, 40.20, 62.76, 71.39, 72.43, 84.68, 88.48, 111.66, 117.05, 117.91, 130.54, 150.11, 151.01, 152.31, 152.91, 159.06; HRMS-CI m/z ($M + 1$) calcd 745.4324, found 743.4325.

4-Amino-5-[2'-(9''-anthracenyl)ethynyl]-1-[2',3',5'-tri-*O*-(*tert*-butyldimethylsilyl)ribofuranosidyl]pyrimidin-4-one (2**).** A solution of **6** (0.260 g, 0.37 mmol) and **7** (0.074 g, 0.37 mmol) in dry diisopropylamine (30 mL) was purged with argon for 10 min. To this solution were added Pd(PPh₃)₂Cl₂ (25 mg, 0.04 mmol) and copper(I) iodide (1.8 mg, 0.009 mmol). The resulting solution was then stirred at room temperature for 12 h. After this period, TLC analysis indicated the presence of a new spot. The solution was concentrated in vacuo and the resulting crude product was purified by column chromatography (silica gel, eluent 1% MeOH in dichloromethane) to afford **2** (70 mg, 24%). UV/vis λ_{max} 368.5 (ϵ 20460), 387 (ϵ 20460), 408 (ϵ 20909). ^1H NMR (300 MHz, CDCl₃): δ 0.04 (s, 3 H), 0.05 (s, 3 H), 0.118 (s, 3 H), 0.124 (s, 3 H), 0.129 (s, 3 H), 0.17 (s, 3 H), 0.77 (s, 9 H), 0.93 (s, 9 H), 0.94 (s, 9 H), 3.8 (d, J = 10.6 Hz, 1 H), 4.04 (d, J = 11.6 Hz, 1 H), 4.13 (m, 2 H), 4.24 (m, 1 H), 5.94 (d, J = 3.6 Hz), 6.19 (bs, 1 H), 7.56 (m, 2 H), 7.62 (m, 2 H), 8.07 (d, J = 8.4 Hz, 2 H), 8.37 (s, 1 H), 8.54 (m, 2 H); ^{13}C NMR (125.5 MHz, CDCl₃): δ -5.16, -4.97, -4.69, -4.19, -4.00, 18.35, 18.38, 18.80, 26.08, 26.35, 62.34, 71.22, 76.92, 84.71, 90.11, 91.42, 91.71, 92.13, 116.47, 126.18, 126.96, 127.38, 129.02, 129.12, 131.54, 133.35, 144.24, 154.64, 165.26. HRMS-CI m/z ($M + 1$) calcd 786.415383, found 786.413762. Anal. Calcd. C₄₃H₆₃N₃O₅-Si₃: C, 65.69; H, 8.07. Found: C, 65.42; H, 8.02.

8-[2'-(9''-Anthracenyl)ethynyl]-1-[2',3',4'-tri-*O*-(*tert*-butyldimethylsilyl)ribofuranosidyl]-2-isobutyrylamidopurin-6-one (10**).** A solution of **7** (1.4 g, 6.9 mmol) and **4** (2.0 g, 2.6 mmol) in dry diisopropylamine (100 mL) was purged with argon for 20 min. To this solution were added Pd(PPh₃)₂Cl₂ (45 mg, 0.064 mmol) and copper(I) iodide (3.0 mg, 0.015 mmol). The resulting solution was then heated under reflux for 12 h. After this period, TLC analysis indicated the presence of a new spot. Accordingly, the solution was concentrated in vacuo and purified by flash chromatography (silica gel, gradient eluent 20–45% ethyl acetate/hexane) to afford **10** (2.0 g, 87%). ^1H NMR (500 MHz, CDCl₃): δ -0.196 (s, 3 H), -0.192 (s, 3 H), -0.138 (s, 3 H), -0.022 (s, 3 H), 0.084 (s, 3 H), 0.090 (s, 3 H), 0.75 (s, 9 H), 0.78 (s, 9 H), 0.85 (s, 9 H), 1.29 (dd, J = 7.0, 2.0 Hz, 6 H), 2.62 (sept, J = 7.0 Hz, 1 H), 3.71 (dd, J = 11.0, 4.5 Hz, 1 H), 3.84 (dd, J = 11.0, 7.5 Hz, 1 H), 4.08 (m, 1 H), 4.46 (dd, J = 11.0, 3.0 Hz, 1 H), 5.19 (dd, J = 6.0, 4.5 Hz, 1 H), 6.30 (d, J = 6.0 Hz, 1 H), 7.50 (m, 2 H), 7.58 (m, 2 H), 8.01 (d, J = 8.6 Hz, 2 H), 8.05 (bs, 1 H), 8.49 (s, 1 H), 8.59 (dd, J = 9.0, 1.0 Hz, 1 H), 12.07 (s, 1 H). ^{13}C NMR (125.5 MHz, CDCl₃): δ -5.65, -5.56, -4.86, -4.53, -4.49, -4.31, 17.86, 18.04, 18.25, 18.85, 19.09, 25.67, 25.74, 25.85, 36.78, 60.37, 62.55, 72.34, 72.83, 85.52, 88.92, 89.41, 92.49, 114.46, 122.75, 125.88, 126.42, 127.54,

128.77, 129.64, 131.03, 133.39, 134.51, 147.22, 147.80, 154.74 177, 92. HRMS-*m/z* (*M* + 1) calcd 896.4634, found 896.4629.

2-Amino-8-[2''-(9'''-anthracenyl)ethynyl]-1-[2',3',4'-tri-*O*-(*tert*-butyldimethylsilyl)ribofuranosidyl]purin-6-one (8). An ice-cold mixture of MeOH/CH₂Cl₂ (3:1; 300 mL) was saturated with ammonia gas. This saturation procedure, involving careful bubbling, was repeated twice. To this solution was added *N*-protected precursor **10** (0.8 g, 0.67 mmol). The resulting clear solution was then stirred at room temperature for 36 h in a sealed flask. The solvents were evaporated off in vacuo. The resulting residue was then purified by column chromatography (silica gel, gradient eluent dichloromethane–3% MeOH in dichloromethane) to afford **8** (0.45 g, 60%). ¹H NMR (500 MHz, CD₂Cl₂): δ –0.34 (s, 3 H), –0.30 (s, 3 H), –0.11 (s, 3 H), –0.03 (s, 3 H), –0.02 (s, 3 H), 0.01 (s, 3 H), 0.56 (s, 9 H), 0.70 (s, 9 H), 0.82 (s, 9 H), 3.60 (dd, *J* = 10.6, 4.8 Hz, 1 H), 3.87 (dd, *J* = 10.7, 8.1 Hz, 1 H), 4.03 (m, 1 H), 4.39 (dd, *J* = 4.4, 2.5 Hz, 1 H), 5.40 ((dd, *J* = 6.3, 4.5 Hz 1 H), 6.27 (d, *J* = 6.3 Hz 1 H), 7.56 (m, 2 H), 7.67 (m, 2 H), 8.09 (d, *J* = 8.5 Hz, 2 H), 8.60 (dd, *J* = 8.7, 0.9 Hz, 1 H), 12.39 (bs, 1 H). ¹³C NMR (125.5 MHz, CD₂Cl₂): δ –5.76, –5.66, –4.81, –4.52, –4.42, –4.36, 18.15, 18.21, 18.24, 25.67, 25.89, 25.94, 63.11, 72.43, 73.05, 86.16, 89.16, 89.76, 91.73, 114.82, 118.81, 126.34, 126.59, 128.13, 129.27, 130.00, 131.53, 132.74, 133.80, 151.85, 154.50, 159.13. HRMS-*m/z* (*M* + 1) calcd 826.4215, found 826.4211.

4-Amino-5-[4''-*N,N*-dimethylaniliny]l]-1-[2',3',5'-tri-*O*-(*tert*-butyldimethylsilyl)ribofuranosidyl]pyrimidin-4-one (9). To a solution of 4-bromo-*N,N*-dimethylaniline **11** (1.0 g, 5.0 mmol) in dry THF (15 mL) at –78 °C was added a solution of BuLi (1.6 M in hexanes, 3.7 mL, 5.9 mmol) slowly. The resulting suspension was then stirred at –78 °C for 30 min. After this period a solution of zinc chloride (1.0 g, 7.4 mmol) in dry THF (15 mL) was added via a cannula. The resulting organozinc intermediate **12** was then allowed to warm to 0 °C over 30 min. In a separate flask a solution of **6** (2.6 g, 3.7 mmol)

in dry toluene (20 mL) was purged with argon for 20 min. To this solution was added Pd(PPh₃)₄ (0.12 g, 0.1 mmol) and the flask was sealed with a septa. The solution of organozinc intermediate **12** was then transferred into this solution via cannula and the resulting mixture was heated under reflux for 12 h. After this period the solvents were evaporated off in vacuo. The crude product was then purified by column chromatography (silica gel, eluent 1:1 EtOAc/hexanes) to afford **9** (1.3 g, 50%). ¹H NMR (500 MHz, CDCl₃): δ –0.17 (s, 3 H), –0.15 (s, 3 H), 0.02 (s, 6 H), 0.04 (s, 3 H), 0.05 (s, 3 H), 0.72 (s, 9 H), 0.85 (s, 9 H), 0.86 (s, 9 H), 2.94 (s, 6 H), 3.66 (dd, *J* = 1.9, 11.3 Hz, 1 H), 3.84 (dd, *J* = 1.9, 11.6 Hz, 1 H), 3.99 (d, *J* = 2.1 Hz, 2 H), 4.15 (m, 1 H), 5.2 (bs, 1 H), 6.01 (d, *J* = 4.8 Hz, 1 H), 6.7 (d, *J* = 7.9 Hz, 2H), 7.07 (d, *J* = 7.9 Hz, 2 H), 7.51 (s, 1 H), 8.2 (bs, 1 H). ¹³C NMR (125.5 MHz, CDCl₃): δ –5.75, –5.56, –4.84, –4.79, –4.47, –4.37, 17.99, 18.04, 18.43, 25.82, 25.85, 26.00, 40.35, 62.59, 71.53, 75.77, 84.39, 88.96, 109.19, 113.08, 120.61, 130.36, 138.84, 150.64, 155.65, 164.93. HRMS-*m/z* (*M* + 1) calcd 705.4263, found 705.4265.

Acknowledgment. Work at The University of Texas at Austin was supported by grants from National Institute of Health (GM 41657) and R. A. Welch Foundation (F-1018). Work at Argonne was supported by the Division of Chemical Sciences, Office of Basic Energy Sciences, US Department of Energy under contract W-31-109-ENG-38.

Supporting Information Available: Steady-state fluorescence titrations between simple anthracene and dimethylaniline, acceptor **2** and “masked donor” **5**, “masked acceptor” **10** and donor **9**, and the plot of ET rate vs *1/T* (PDF). This material is available free of charge via the Internet at <http://pubs.acs.org>.

JA005547S